

## ON-/OFF-STATE DESIGN OF SEMICONDUCTOR DOPING PROFILES\*

MARTIN BURGER<sup>†</sup>, RENÉ PINNAU<sup>‡</sup>, AND MARIE-THERESE WOLFRAM<sup>§</sup>

**Abstract.** We consider the multi-objective optimal dopant profiling of semiconductor devices. The two objectives are to gain a higher on-state current while the off-state current is kept small. This design question is treated as a constrained optimization problem, where the constraints are given by the stationary drift-diffusion model for the on-state and the linearized drift-diffusion model for the off-state. Using the doping profile as a state variable and the electrostatic potential as the new design variable, we obtain a simpler optimization problem, whose Karush-Kuhn-Tucker conditions partially decouple. Based on this observation we can construct a very efficient iterative optimization algorithm, which avoids solving the fully coupled drift-diffusion system. Due to the simple structure of the adjoint equations, this algorithm can be easily included into existing semiconductor simulation tools. The efficiency and success of this multi-objective design approach is underlined by various numerical examples.

**Key words.** Semiconductor design, drift-diffusion model, Gummel iteration, optimal control, multi-objective, dopant profiling.

**AMS subject classifications.** 35J50, 49J20, 49K20.

### 1. Introduction

Optimal design problems for semiconductor devices are receiving growing attention in modern microelectronics, and due to the ongoing advances in miniaturization, mathematical optimization methods play an increasingly important role (cf. e.g. [20, 23, 24, 25, 6, 12, 13]). The major goal of optimal semiconductor design is to improve the device characteristics, in particular, current flows over some contact by designing a suitable device doping profile (representing the density of ion impurities within the material). In mathematical terms, this leads (at the coarsest level of device models) to a distributed optimal control problem for a system of partial differential equations, the so-called *drift-diffusion system*, in which the doping profile enters as a source term. The mathematical analysis and the construction of numerical optimization algorithms for the on-state design based on the drift-diffusion model has been thoroughly studied [12, 13, 6, 15, 14, 4]. Recently, even extensions to the the energy-transport model have become available [8, 9, 10].

The aim of this paper is the numerical solution of optimal design problems which involve on- and off-states, i.e., a state with large applied voltage (on-state) and a second at equilibrium with possible voltage fluctuations (off-state) [25, 23]. The typical design goal in such cases is to maximize the on-state current while keeping the off-state current (which can actually be a leakage current) small. By achieving this design goal, the practical performance of the device can be improved without increasing the losses when the device is switched off.

In the mathematical literature, there exist two different approaches to optimal

---

\*Received: June 25, 2008; accepted (in revised version): October 14, 2008. Communicated by Pierre Degond.

<sup>†</sup>Institut für Numerische und Angewandte Mathematik, Westfälische Wilhelms-Universität Münster, Einsteinstr. 62, 48149 Münster, Germany (martin.burger@uni-muenster.de).

<sup>‡</sup>Fachbereich Mathematik, Technische Universität Kaiserslautern, (pinnau@mathematik.uni-kl.de).

<sup>§</sup>Johann Radon Institute for Computational and Applied Mathematics (Austrian Academy of Sciences), Altenbergerstr. 69, 4040 Linz, Austria (marietherese.wolfram@oeaw.ac.at).

dopant profiling, which differ in the respective choice of the design variable. Either the doping profile is directly used (cf. [15, 4, 28] and the references therein), or one uses the total charge density (cf. [6, 8] and the references therein). Here, we will follow the second choice and extend the fast Gummel iteration for the on-state design presented in [6, 7] to the multi-objective on-/off-state design. The algorithm relies on a convex combination of the two design goals followed by the iterative solution of the respective optimality system. This yields a fast numerical method which avoids the computation of Pareto sets (see e.g. [21] for a survey on mathematical approaches to multiobjective optimization)

The paper is organized as follows. In the remainder of this section we introduce the underlying model equations for the optimal on-/off-state design of the doping profile, which is given by the stationary drift-diffusion model. The optimization problem is introduced and analyzed in section 2. In particular, we suggest a linearized treatment of the off-state and we prove the existence of a minimizer and derive the first-order optimality system. A fast iterative procedure generalizing the classical Gummel iteration for the forward problem is introduced in section 3. In section 4, we present numerical results for the on-/off-state design of different semiconductor devices. Concluding remarks are given in section 5.

**1.1. The drift-diffusion model.** The stationary drift-diffusion system in physical variables consists of nonlinear elliptic equations for the electrostatic potential  $V$ , the electron density  $n$ , and the hole density  $p$  [17, 18]:

$$\begin{aligned} \operatorname{div}(\epsilon_s \nabla V) &= q(n - p - C) && \text{in } \Omega, \\ \operatorname{div}(D_n \nabla n - \mu_n n \nabla V) &= 0 && \text{in } \Omega, \\ \operatorname{div}(D_p \nabla p + \mu_p p \nabla V) &= 0 && \text{in } \Omega, \end{aligned}$$

where  $\epsilon_s$  denotes the semiconductor permittivity,  $q$  the elementary charge,  $\mu_n$  and  $\mu_p$  are the electron and hole mobilities, and  $D_n$  and  $D_p$  are the electron and hole diffusion coefficients, respectively. This system is supplemented by a homogeneous Neumann boundary condition on a part of the boundary  $\partial\Omega_N$ , modeling the insulating parts of the boundary, and Dirichlet conditions on the remaining part, which models the Ohmic contacts of the device:

$$\begin{aligned} V(x) = V_D(x) &= U(x) + V_{bi}(x) = U(x) + U_T \ln\left(\frac{n_D(x)}{n_i}\right) && \text{on } \partial\Omega_D, \\ n(x) = n_D(x) &= \frac{1}{2} \left( C(x) + \sqrt{C(x)^2 + 4n_i^2} \right) && \text{on } \partial\Omega_D, \\ p(x) = p_D(x) &= \frac{1}{2} \left( -C(x) + \sqrt{C(x)^2 + 4n_i^2} \right) && \text{on } \partial\Omega_D. \end{aligned}$$

Here  $n_i$  is the intrinsic density,  $U_T$  the thermal voltage, and  $U$  is the applied biasing voltage.

Under usual conditions, the mobilities and diffusion coefficients are related by Einstein's relation, i.e.,  $D_{n/p} = \mu_{n/p} U_T$ . which enables the transformation into the so-called *Slotboom variables* [22] defined by

$$n = n_i e^{V/U_T} u, \quad p = n_i e^{-V/U_T} v. \tag{1.1}$$

The assumptions that  $\epsilon_s$  and  $q$  are constant allows for the choice of an appropriate

scaling, yielding the system

$$\lambda^2 \Delta V = \delta^2 (e^V u - e^{-V} v) - C \quad \text{in } \Omega, \quad (1.2a)$$

$$\operatorname{div}(\mu_n e^V \nabla u) = 0 \quad \text{in } \Omega, \quad (1.2b)$$

$$\operatorname{div}(\mu_p e^{-V} \nabla v) = 0 \quad \text{in } \Omega, \quad (1.2c)$$

where  $\lambda^2 = (\epsilon_s U_T) / (q C_{\max} L^2)$  is the scaled Debye length of the device (for details see, e.g., [18]) and  $\delta^2 = \frac{n_i}{C_{\max}}$ . For brevity we shall use a scaling such that  $\delta = 1$  in the subsequent presentation. For simplicity we shall use the Dirichlet boundary conditions, which can be written as

$$V = V_D = U + V_{bi} \quad \text{on } \partial\Omega_D, \quad (1.2d)$$

$$u = u_D \quad \text{on } \partial\Omega_D, \quad (1.2e)$$

$$v = v_D \quad \text{on } \partial\Omega_D, \quad (1.2f)$$

where  $u_D$  and  $v_D$  are the transformations of  $n_D$  and  $v_D$  under (1.1). On the remaining part  $\partial\Omega_N = \partial\Omega \setminus \partial\Omega_D$ , the homogeneous Neumann conditions can be formulated on  $J_n$  and  $J_p$ , where  $J_n$  and  $J_p$  are the electron and hole current densities, which are related to the Slotboom variables by

$$J_n = \mu_n e^V \nabla u, \quad J_p = -\mu_p e^{-V} \nabla v. \quad (1.2g)$$

Hence, we have

$$\frac{\partial V}{\partial \nu} = 0 \quad \text{on } \partial\Omega_N, \quad (1.2h)$$

$$\frac{\partial u}{\partial \nu} = 0 \quad \text{on } \partial\Omega_N, \quad (1.2i)$$

$$\frac{\partial v}{\partial \nu} = 0 \quad \text{on } \partial\Omega_N. \quad (1.2j)$$

Throughout the whole paper, we shall assume that all Dirichlet boundary values  $V_D$ ,  $u_D$ , and  $v_D$ , are bounded in  $H^{\frac{1}{2}}(\Omega) \cap L^\infty(\Omega)$ , which is the basis for an existence proof of the drift-diffusion system in  $(H^1(\Omega) \cap L^\infty(\Omega))^3$  [18]. For notational simplicity we further assume that  $\mu_n = \mu_p = 1$ .

## 2. The optimal design problem

The design problem under investigation involves the on-state and the off-state of the device, i.e., we encounter a typical problem of multi-objective optimization. In general, one is interested in an increased on-state current while the off-state current is kept as small as possible. This allows for a better device performance in the on-state without increasing the so-called leakage-current in the off-state. Our optimization approach is essentially based on a combined least-squares formulation of both optimization goals.

One objective of the optimization, the on-state current flow over a contact  $\Gamma$ , is given by

$$I = \int_{\Gamma} J d\nu = \int_{\Gamma} (J_n + J_p) d\nu, \quad (2.1)$$

where  $J_n$  and  $J_p$  are computed from the drift-diffusion model (1.2) for a specific onstate biasing voltage  $U = U_{\text{on}}$ .

Since the off-state is in general a fluctuation near the thermal equilibrium state (given for  $U = 0$ , where no current flows) and is not exactly known, we do not prescribe a specific offstate voltage  $U_{\text{off}}$ . Instead we intend to minimize the slope of the current voltage characteristics (IVC), i.e., we try to keep

$$K := \frac{dI}{dU}(0)$$

small, which actually suffices to guarantee small leakage currents. We shall see below that  $K$  can be easily calculated from the linearized drift-diffusion model. This leads finally to the minimization of an objective functional of the form

$$Q(I, K) = Q_1(I) + \omega Q_2(K), \tag{2.2}$$

where  $I$  and  $K$  are defined via PDE constraints. Here,  $\omega$  is a nonnegative weighting parameter, which allows for the adjustment of the two design goals.

**2.1. On-state and off-state.** The on-state is clearly given by a solution of (1.2) for  $U = U_{\text{on}}$  in (1.2d), from which we can directly compute  $I$ .

To compute the current slope  $K$ , we use a linearization around the thermal equilibrium state  $(u_0, v_0, V_0)$ , which is given by  $u_0 = v_0 \equiv 1$  and

$$\lambda^2 \Delta V_0 = e^{V_0} - e^{-V_0} - C \quad \text{in } \Omega, \tag{2.3a}$$

$$V_0 = V_{bi} \quad \text{on } \partial\Omega_D, \tag{2.3b}$$

$$\frac{\partial V_0}{\partial \nu} = 0 \quad \text{on } \partial\Omega_N. \tag{2.3c}$$

REMARK 2.1. For an analytical discussion of the linearized drift-diffusion model we refer to [17, 18] and the references therein. Note, that the nonlinear Poisson-Boltzmann equation allows for a unique weak solution.

Then,  $K$  is calculated via

$$K = K_n + K_p, \quad K_n = e^{V_0} \nabla u_1, \quad K_p = -e^{-V_0} \nabla v_1, \tag{2.4}$$

where  $u_1$  and  $v_1$  are defined as the solutions of the carrier continuity equations

$$\text{div}(e^{V_0} \nabla u_1) = 0 \quad \text{in } \Omega, \tag{2.5a}$$

$$\text{div}(e^{-V_0} \nabla v_1) = 0 \quad \text{in } \Omega, \tag{2.5b}$$

with boundary conditions

$$u_1 = -h, \quad v_1 = h \quad \text{on } \partial\Omega_D \tag{2.5c}$$

and

$$\frac{\partial u_1}{\partial \nu} = 0, \quad \frac{\partial v_1}{\partial \nu} = 0 \quad \text{on } \partial\Omega_N. \tag{2.5d}$$

REMARK 2.2. Note that the system for the off-state fully decouples, which is one of the main ingredients for the construction of the upcoming iterative solution procedure. This is an effect of the special choice of the Slotboom variables. For the standard drift-diffusion model in the variables  $(n, p, V)$  one would get a fully coupled system instead.

**2.2. Design goal and stabilization.** Typically, one is interested in an increase of the on-state outflow current  $I$ . This can be achieved by minimizing either

$$Q_1(I) = -I$$

or

$$Q_1(I) = \frac{1}{2}|I - I^*|^2, \quad (2.6)$$

where  $I^*$  is some desired outflow current [4].

The easiest way to keep the off-state current small is to minimize

$$Q_2(K) = \frac{1}{2}K^2. \quad (2.7)$$

The standard design variable is the doping profile  $C$ . The adjoint approach used in [13] yields satisfying results at moderate numerical costs. There, the optimization of the on-state current is done by a minimization of a functional of the form

$$Q_\beta(C) := Q(n(C), p(C), V(C)) + \frac{\beta}{2}\|C - C^*\|^2 \rightarrow \min_C, \quad (2.8)$$

where  $C^*$  is a given doping profile.

A different approach for the on-state design was introduced in [6] and recently analytically investigated in [7]. There, the interpretations of control and state were exchanged between doping profile  $C$  and the potential  $V$ . Hence, the potential  $V$  is used as the new design variable and the Poisson Equation (1.2a) is interpreted as a state equation for the doping profile  $C$ .

In the following, we generalize this approach to our multi-objective design problem. Again, we introduce a new penalty term dependent on  $V - V^*$  rather than on  $C - C^*$ . For the initial guess  $V^*$  we use the one obtained from the solution of the on-state drift-diffusion system (1.2) with doping profile  $C^*$ . Since the Laplacian of  $V - V^*$  is needed for the evaluation of  $C - C^*$ , it seems natural to use a penalty term dependent on the rescaled charge density

$$W := \Delta(V - V^*), \quad (2.9)$$

i.e., we intend to minimize the functional

$$Q_\epsilon(I, K, W) := Q(I, K) + \frac{\epsilon}{2} \int_\Omega |W(x)|^2 dx \quad (2.10)$$

subject to (2.9), the on-state drift-diffusion system (1.2), and the off-state system (2.5). In order to ensure that  $C$  does not change its boundary values,  $W$  must satisfy homogeneous boundary conditions on  $\partial\Omega_D$ , and on the remaining boundary we may use any homogeneous boundary condition. For simplicity we will carry out our analysis for

$$W = 0 \quad \text{on } \partial\Omega. \quad (2.11)$$

Analogous treatment is possible for homogeneous Neumann conditions  $\frac{\partial W}{\partial \nu} = 0$  on  $\partial\Omega_N$ . The Neumann condition can be favorable with respect to implementation, since, as we shall see below, this will yield a Poisson equation for  $W$  with the same type of boundary conditions as for  $V$ , hence the same solver can be used.

REMARK 2.3. The numerical results in [13, 6] show that the increase of the on-state current goes in general hand-in-hand with an increase of the off-state current. This is due to the fact that the higher on-state current is achieved by a larger doping concentration, resulting in more free carriers in the device. But this leads directly to an increase of the leakage current. Thus, a multi-objective design approach seems necessary. Note that our two design goals are competitive, which increases the numerical difficulties significantly.

**2.3. Existence of a minimizer.** In the following we analytically investigate the optimization problem

$$Q_\epsilon(I, K, W) \rightarrow \min_{(u, v, u_1, v_1, V, V_0, W) \in \mathcal{D}_{ad}}, \tag{2.12}$$

with the admissible domain

$$\mathcal{D}_{ad} := \{(u, v, u_1, v_1, V, V_0, W) \in H^1(\Omega)^4 \times (H^1(\Omega) \cap L^\infty(\Omega))^2 \times L^2(\Omega) \text{ satisfying (1.2b)-(1.2j), (2.5), (2.3), (2.9)}\}.$$

THEOREM 2.4. (Existence) *Let  $\epsilon > 0$  be given. Then there exists a minimizer*

$$(\bar{u}, \bar{v}, \bar{u}_1, \bar{v}_1, \bar{V}, \bar{V}_0, \bar{W}) \in H^1(\Omega)^4 \times (H^1(\Omega) \cap L^\infty(\Omega))^2 \times L^2(\Omega) \tag{2.13}$$

of the constrained minimization problem (2.12).

*Proof.* Suppose  $(u^k, v^k, u_1^k, v_1^k, V^k, V_0^k, W^k)_{k \in \mathbb{N}}$  is a minimizing sequence, then the coercivity of  $Q_\epsilon$  with respect to  $W$  ensures that  $(W^k)_{k \in \mathbb{N}}$  is uniformly bounded in  $L^2(\Omega)$ .

Thus, by standard elliptic regularity [26],  $(V^k - V^*)_{k \in \mathbb{N}}$  is uniformly bounded in  $H^2(\Omega) \hookrightarrow C(\bar{\Omega})$ . Since the a-priori guess  $V^*$  is in  $L^\infty(\Omega)$ , we obtain uniform boundedness of  $(V^k)_{k \in \mathbb{N}}$  in  $L^\infty(\Omega)$ . Standard energy arguments for the elliptic equations (1.2b) and (1.2c) consequently yield the boundedness of  $(u^k)_{k \in \mathbb{N}}$  and  $(v^k)_{k \in \mathbb{N}}$  in  $H^1(\Omega) \cap L^\infty(\Omega)$ .

From

$$C = C^* - \lambda^2 W + e^V u - e^{V^*} u^* - e^{-V} v + e^{-V^*} v^*$$

we get, using (2.3a),

$$\lambda^2 \Delta V_0^k = e^{V_0^k} - e^{-V_0^k} - \left( C^* - \lambda^2 W^k + e^{V^k} u^k - e^{V^*} u^* - e^{-V^k} v^k + e^{-V^*} v^* \right). \tag{2.14}$$

This monotone equation admits a unique solution  $V_0^k \in H^1(\Omega) \cap L^\infty(\Omega)$ , which depends Lipschitz continuously on the right-hand side [18, Lem. 3.3.14]. Thus, also  $(V_0^k)_{k \in \mathbb{N}}$  is uniformly bounded in  $H^1(\Omega) \cap L^\infty(\Omega)$ .

Again, standard estimates for the elliptic equations (2.5) yield the boundedness of  $(u_1^k)_{k \in \mathbb{N}}$  and  $(v_1^k)_{k \in \mathbb{N}}$  in  $H^1(\Omega) \cap L^\infty(\Omega)$ .

Thus, we can extract a weakly converging subsequence, again denoted by

$$(u^k, v^k, u_1^k, v_1^k, V^k, V_0^k, W^k)_{k \in \mathbb{N}} \in H^1(\Omega)^4 \times H^1(\Omega)^2 \times L^2(\Omega),$$

which also preserves the  $L^\infty$  bound (and such that  $\Delta(V^k - V^*)$  converges weakly in  $L^2(\Omega)$ ). The weak closedness of the admissible domain and the weak lower semicontinuity of the objective functional imply that the weak limit of this subsequence is a minimizer of (2.12).  $\square$

**2.4. First-order optimality.** For the following analysis it is most convenient to eliminate  $C$  in (2.3a) by (1.2a) and to introduce the new variable  $\psi = V_0 - V$ . This yields the equation

$$\lambda^2 \Delta \psi = e^V (e^\psi - u) - e^{-V} (e^{-\psi} - v) \quad \text{in } \Omega, \tag{2.15}$$

$$\psi = -U \quad \text{on } \partial\Omega_D, \tag{2.16}$$

$$\frac{\partial \psi}{\partial \nu} = 0 \quad \text{on } \partial\Omega_N. \tag{2.17}$$

For notational convenience we define the vector of state variables  $y := (u, v, u_1, v_1, V, \psi)$  and the vector of Lagrange multipliers  $\mu := (\mu_1, \mu_2, \mu_3, \mu_4, \mu_5, \mu_6)$ . In order to derive the first-order optimality conditions, we define the Lagrangian  $\mathcal{L} : \mathcal{D}_{ad} \times H^1(\Omega)^6 \rightarrow \mathbb{R}$ , given by

$$\begin{aligned} \mathcal{L}(y, W; \mu) := & Q_\epsilon(I(y, W), K(y, W)) + \int_\Omega (e^V \nabla u \nabla \mu_1 - e^{-V} \nabla v \nabla \mu_2) \, dx \\ & + \int_\Omega (e^{V+\psi} \nabla u_1 \nabla \mu_3 - e^{-(V+\psi)} \nabla v_1 \nabla \mu_4) \, dx \\ & + \int_\Omega \lambda^2 \nabla \psi \nabla \mu_5 + [e^V (e^\psi - u) - e^{-V} (e^{-\psi} - v)] \mu_5 \, dx \\ & + \int_\Omega (\nabla(V - V^*) \nabla \mu_6 + W \mu_6) \, dx. \end{aligned} \tag{2.18}$$

Due to  $V, \psi \in H^1(\Omega) \cap L^\infty(\Omega)$  and  $(u, v) \in H^1(\Omega)^2$  one can easily verify the Fréchet-differentiability of  $\mathcal{L}$ .

**PROPOSITION 2.5.** *The Lagrangian  $\mathcal{L}$  is continuously Fréchet-differentiable on  $\mathcal{D}_{ad} \times H^1(\Omega)^6$ .*

Each solution of the optimization problem is a saddle point of the Lagrangian, i.e., a solution of

$$\inf_{(y, W)} \sup_{\mu} \mathcal{L}(y, W, \mu). \tag{2.19}$$

For such saddle-points we can derive the Karush-Kuhn-Tucker conditions by computing the variations of the Lagrangian  $\mathcal{L}$  with respect to the primal and dual variables, which all must vanish. The variations with respect to the dual variables just yield the equality constraints, while from the variation with respect to the primal variables we deduce that

$$0 = \frac{\partial}{\partial u} Q_\epsilon(y, W) \hat{u} + \int_\Omega e^V \nabla \hat{u} \cdot \nabla \mu_1 \, dx - \int_\Omega \hat{u} e^V \mu_5 \, dx, \tag{2.20a}$$

$$0 = \frac{\partial}{\partial v} Q_\epsilon(y, W) \hat{v} - \int_\Omega e^{-V} \nabla \hat{v} \cdot \nabla \mu_2 \, dx + \int_\Omega \hat{v} e^{-V} \mu_5 \, dx, \tag{2.20b}$$

$$0 = \frac{\partial}{\partial u_1} Q_\epsilon(y, W) \hat{u}_1 + \int_\Omega (e^{V+\psi} \nabla \hat{u}_1 \cdot \nabla \mu_3) \, dx, \tag{2.20c}$$

$$0 = \frac{\partial}{\partial v_1} Q_\epsilon(y, W) \hat{v}_1 - \int_\Omega (e^{-(V+\psi)} \nabla \hat{v}_1 \cdot \nabla \mu_4) \, dx, \tag{2.20d}$$

$$\begin{aligned}
0 &= \frac{\partial}{\partial \psi} Q_\epsilon(y, W) \hat{\psi} + \int_{\Omega} \hat{\psi} \left( e^{V+\psi} \nabla u_1 \cdot \nabla \mu_3 + e^{-(V+\psi)} \nabla v_1 \nabla \mu_4 \right) dx \\
&\quad + \int_{\Omega} \lambda^2 \nabla \hat{\psi} \cdot \nabla \mu_5 + \hat{\psi} \left( e^{V+\psi} + e^{-(V+\psi)} \right) \mu_5 dx, \tag{2.20e}
\end{aligned}$$

$$\begin{aligned}
0 &= \frac{\partial}{\partial V} Q_\epsilon(y, W) \hat{V} + \int_{\Omega} \hat{V} \left( e^V \nabla u \cdot \nabla \mu_1 + e^{-V} \nabla v \nabla \mu_2 \right) + \nabla \hat{V} \cdot \nabla \mu_6 dx \\
&\quad + \int_{\Omega} \hat{V} \left( e^{V+\psi} \nabla u_1 \nabla \mu_3 + e^{-(V+\psi)} \nabla v_1 \nabla \mu_4 \right) dx \\
&\quad + \int_{\Omega} \hat{V} \left( e^V (e^\psi - u) + e^{-V} (e^{-\psi} - v) \right) \mu_5 dx, \tag{2.20f}
\end{aligned}$$

$$0 = \int_{\Omega} \hat{W} (\epsilon W + \mu_6) dx, \tag{2.20g}$$

hold for all variations  $(\hat{u}, \hat{v}, \hat{u}_1, \hat{v}_1, \hat{V}, \hat{\psi}, \hat{W}) \in H^1(\Omega)^6 \times L^2(\Omega)$ .

Note that the so-called *adjoint system* (2.20) has a simple triangular structure with respect to the Lagrangian variables  $\mu$ . For given primal variables  $y$  we can solve consecutively for  $\mu_3, \mu_4$  followed by  $\mu_5$  and  $\mu_1, \mu_2$  and finally  $\mu_6$ . Thus, the problem of proving existence and uniqueness of Lagrangian variables  $\mu \in H_{0,D}^1(\Omega)^6$  solving (2.20) for given primal variables  $y$ , simplifies to analyzing subsequently six different linear variational problems, which turn out to be coercive (also compare this with the existence proof in [6]).

**THEOREM 2.6.** *Let  $(y, W) \in \mathcal{D}_{ad}$  be given. Then there exists a unique solution  $\mu \in H_{0,D}^1(\Omega)^6$  of the variational problem (2.20).*

**REMARK 2.7.** This yields another advantage of our approach with respect to the direct optimal control approach, where analyzing the adjoint problem is a difficult task, which is possible only close to thermal equilibrium (cf. [13]). In general, existence of Lagrange multipliers is not guaranteed.

To derive the strong form the adjoint equations we proceed by computing the partial derivatives of  $Q_\epsilon$ . We get

$$Q'_1(u, v, V)(\hat{u}, \hat{v}, \hat{V}) = (I - I^*) \int_{\Gamma} \left( e^V \frac{\partial \hat{u}}{\partial \nu} - e^{-V} \frac{\partial \hat{v}}{\partial \nu} \right) ds \tag{2.21}$$

and

$$Q'_2(u_1, v_2, \psi)(\hat{u}_1, \hat{v}_1, \hat{\psi}) = K \int_{\Gamma} \left( e^{V+\psi} \frac{\partial \hat{u}_1}{\partial \nu} - e^{-(V+\psi)} \frac{\partial \hat{v}_1}{\partial \nu} \right) ds. \tag{2.22}$$

If we choose the Lagrangian variables  $\mu_i$ ,  $i = 1, 2$  such that  $\mu_i = 0$  only on  $\partial\Omega_D \setminus \Gamma$  and  $\mu_1 = \mu_2 = \eta$  on  $\Gamma$  for some real constant  $\eta$ , then we can derive a simple form of the optimality system. With this choice, the Lagrangian becomes

$$\begin{aligned}
\mathcal{L}(y, W; \mu) &= Q_\epsilon(I(y, W), K(y, W)) + \int_{\Omega} \left( e^V \nabla u \nabla \mu_1 - e^{-V} \nabla v \nabla \mu_2 \right) dx \\
&\quad + \int_{\Omega} \left( e^{V+\psi} \nabla u_1 \nabla \mu_3 - e^{-(V+\psi)} \nabla v_1 \nabla \mu_4 \right) dx \\
&\quad + \int_{\Omega} \lambda^2 \nabla \psi \nabla \mu_5 + [e^V (e^\psi - u) - e^{-V} (e^{-\psi} - v)] \mu_5 dx \\
&\quad + \int_{\Omega} (\nabla(V - V^*) \nabla \mu_6 + W \mu_6) dx - \eta I. \tag{2.23}
\end{aligned}$$

and the optimality with respect to  $u$  yields

$$(I - I^* - \eta) \int_{\Gamma} \left( e^V \frac{\partial \hat{u}}{\partial \nu} \right) ds + \int_{\Omega} (e^V \nabla \hat{u} \cdot \nabla \mu_1) dx + - \int_{\Omega} \hat{u} e^V \mu_5 dx = 0. \quad (2.24)$$

With the choice  $\eta = I - I^*$ , this reduces to the weak formulation corresponding to the elliptic partial differential equation

$$\operatorname{div}(e^V \nabla \mu_1) = -e^V \mu_5 \quad \text{in } \Omega, \quad (2.25a)$$

subject to the boundary conditions

$$\mu_1 = I - I^* \quad \text{on } \Gamma, \quad (2.25b)$$

$$\mu_1 = 0 \quad \text{on } \partial\Omega_D \setminus \Gamma, \quad (2.25c)$$

$$\frac{\partial \mu_1}{\partial \nu} = 0 \quad \text{on } \partial\Omega_N. \quad (2.25d)$$

Analogous reasoning yields the equation

$$\operatorname{div}(e^{-V} \nabla \mu_2) = -e^{-V} \mu_5 \quad \text{in } \Omega, \quad (2.26a)$$

subject to the boundary conditions

$$\mu_2 = -(I - I^*) \quad \text{on } \Gamma, \quad (2.26b)$$

$$\mu_2 = 0 \quad \text{on } \partial\Omega_D \setminus \Gamma, \quad (2.26c)$$

$$\frac{\partial \mu_2}{\partial \nu} = 0 \quad \text{on } \partial\Omega_N. \quad (2.26d)$$

Next, we choose the Lagrangian variables  $\mu_i$ ,  $i = 3, 4$  such that  $\mu_i = 0$  only on  $\partial\Omega_D \setminus \Gamma$  and  $\mu_3 = \mu_4 = \rho$  on  $\Gamma$  for some real constant  $\rho$ . With this choice, the Lagrangian becomes

$$\begin{aligned} \mathcal{L}(y, W; \mu) &= Q_{\epsilon}(I(y, W), K(y, W)) + \int_{\Omega} (e^V \nabla u \nabla \mu_1 - e^{-V} \nabla v \nabla \mu_2) dx \\ &+ \int_{\Omega} \left( e^{V+\psi} \nabla u_1 \nabla \mu_3 - e^{-(V+\psi)} \nabla v_1 \nabla \mu_4 \right) dx \\ &+ \int_{\Omega} \lambda^2 \nabla \psi \nabla \mu_5 + [e^V (e^{\psi} - u) - e^{-V} (e^{-\psi} - v)] \mu_5 dx \\ &+ \int_{\Omega} (\nabla(V - V^*) \nabla \mu_6 + W \mu_6) dx - \rho K, \end{aligned} \quad (2.27)$$

and the optimality with respect to  $u_1$  yields

$$(K - \rho) \int_{\Gamma} \left( e^{V+\psi} \frac{\partial \hat{u}_1}{\partial \nu} \right) ds + \int_{\Omega} (e^{V+\psi} \nabla \hat{u}_1 \cdot \nabla \mu_3) dx = 0. \quad (2.28)$$

With the choice  $\rho = K$ , this reduces to the weak formulation of

$$\operatorname{div}(e^{V+\psi} \nabla \mu_3) = 0 \quad \text{in } \Omega, \quad (2.29a)$$

subject to the boundary conditions

$$\mu_3 = K \quad \text{on } \Gamma, \quad (2.29b)$$

$$\mu_3 = 0 \quad \text{on } \partial\Omega_D \setminus \Gamma, \quad (2.29c)$$

$$\frac{\partial \mu_3}{\partial \nu} = 0 \quad \text{on } \partial\Omega_N. \quad (2.29d)$$

Repeating the argument, we get the equation

$$\operatorname{div} \left( e^{-(V+\psi)} \nabla \mu_4 \right) = 0 \quad \text{in } \Omega, \tag{2.30a}$$

subject to the boundary conditions

$$\mu_4 = -K \quad \text{on } \Gamma, \tag{2.30b}$$

$$\mu_4 = 0 \quad \text{on } \partial\Omega_D \setminus \Gamma, \tag{2.30c}$$

$$\frac{\partial \mu_4}{\partial \nu} = 0 \quad \text{on } \partial\Omega_N. \tag{2.30d}$$

Further, the optimality with respect to  $\psi$  is the variational formulation of the elliptic equation

$$-\lambda^2 \Delta \mu_5 + \left( e^{V+\psi} + e^{-(V+\psi)} \right) \mu_5 = -K_n \cdot \nabla \mu_3 - K_p \cdot \nabla \mu_4 \quad \text{in } \Omega, \tag{2.31a}$$

subject to the boundary conditions

$$\mu_5 = 0 \quad \text{on } \partial\Omega_D, \tag{2.31b}$$

$$\frac{\partial \mu_5}{\partial \nu} = 0 \quad \text{on } \partial\Omega_N. \tag{2.31c}$$

The optimality with respect to  $V$  is the variational formulation of the elliptic equation

$$-\Delta \mu_6 + \left( e^V (e^\psi - u) + e^{-V} (e^{-\psi} - v) \right) \mu_5 = -K_n \cdot \nabla \mu_3 - K_p \cdot \nabla \mu_4 - J_n \cdot \nabla \mu_1 - J_p \cdot \nabla \mu_2 \quad \text{in } \Omega, \tag{2.32a}$$

subject to the boundary conditions

$$\mu_6 = 0 \quad \text{on } \partial\Omega_D, \tag{2.32b}$$

$$\frac{\partial \mu_6}{\partial \nu} = 0 \quad \text{on } \partial\Omega_N. \tag{2.32c}$$

Finally, we determine the optimality condition with respect to  $W$ , which can be rewritten as the equation

$$\epsilon W = -\mu_6 \quad \text{in } \Omega. \tag{2.33}$$

REMARK 2.8. The simple form of (2.33) allows for the elimination of the adjoint variable  $\mu_6$ .

### 3. The generalized Gummel iteration

In the following we present an iterative procedure motivated by the classical Gummel iteration for the solution of the drift-diffusion model [11]. This results in a full decoupling of the KKT systems, such that only a sequence of elliptic equations needs to be solved. This approach was already successfully used for the on-state design in [6] and analytically investigated in [7].

Standard techniques for the computation of a minimizer of (2.12), like gradient descent or Newton’s method for the KKT system (2.20), require the consecutive solution of the state and of the adjoint system, which is in general non-elliptic due to the strong influence of first-order terms (compare also [12, 13]). Of course, fixed-point

iterations that consecutively solve single elliptic equations can also be constructed for KKT systems in quite arbitrary optimization models. However, such approaches usually do not lead to descent in the objective functional and are hence difficult to globalize. If at all, convergence can be achieved via strong damping, which may result in a very slow iterative scheme.

Instead, we exploit the triangular structure of the adjoint system and use a lower triangular approximation of the optimality system. We first solve equation (2.9) with given  $W$  for the potential  $V$ , and subsequently the continuity equations (1.2b)–(1.2c) with given potential  $V$  for  $u$  and  $v$ . Using this data we can solve (2.15) for the linearized potential  $\psi$  followed by the solution of (2.5) for  $u_1$  and  $v_1$ . With given state variables, we solve the adjoint equations (2.29a)–(2.30a) to obtain the Lagrangian variables  $\mu_3$  and  $\mu_4$ . Then we can solve (2.31a) for  $\mu_5$ , followed by the solution of (2.25a)–(2.26a) for  $\mu_1$  and  $\mu_2$ . Finally, we can compute  $\mu_6$  from (2.32a) and update  $W$  via (2.33).

All together, we can write this iteration as

ALGORITHM 3.1.

1. Choose  $W^0$ .
2. For  $k=1,2,\dots$ , consecutively solve

$$\begin{aligned} \Delta V^k &= \Delta V^* + W^{k-1} \\ \operatorname{div} (e^{V^k} \nabla u^k) &= 0 \\ \operatorname{div} (e^{-V^k} \nabla v^k) &= 0 \\ \lambda^2 \Delta \psi^k &= e^{V^k} (e^{\psi^k} - u^k) - e^{-V^k} (e^{-\psi^k} - v^k) \\ \operatorname{div} (e^{V^k + \psi^k} \nabla u_1^k) &= 0 \\ \operatorname{div} (e^{-(V^k + \psi^k)} \nabla v_1^k) &= 0 \\ \operatorname{div} (e^{V^k + \psi^k} \nabla \mu_3^k) &= 0 \\ \operatorname{div} (e^{-(V^k + \psi^k)} \nabla \mu_4^k) &= 0 \\ -\lambda^2 \Delta \mu_5^k + (e^{V^k + \psi^k} + e^{-(V^k + \psi^k)}) \mu_5^k &= -K_n^k \cdot \nabla \mu_3^k - K_p^k \cdot \nabla \mu_4^k \\ \operatorname{div} (e^{V^k} \nabla \mu_1^k) &= -e^{V^k} \mu_5^k \\ \operatorname{div} (e^{-V^k} \nabla \mu_2^k) &= -e^{-V^k} \mu_5^k \\ -\Delta \mu_6^k + (e^{V^k} (e^{\psi^k} - u^k) + e^{-V^k} (e^{-\psi^k} - v^k)) \mu_5^k &= \\ &= -K_n^k \cdot \nabla \mu_3^k - K_p^k \cdot \nabla \mu_4^k - J_n^k \cdot \nabla \mu_1^k - J_p^k \cdot \nabla \mu_2^k \\ \epsilon W^k &= -\mu_6^k \end{aligned}$$

subject to the above boundary conditions.

With this generalized Gummel iteration we mainly need to solve linear Poisson and continuity equations and hence we can use all building blocks of typical device simulators. The only nonlinear equation is the third one for  $\psi^k$ , which is actually a Poisson-Boltzmann equation in equilibrium and can be solved efficiently via a Newton iteration.

REMARK 3.2. The corresponding value of the doping profile can be computed independently by

$$C^k - C^* = -\lambda^2 W^k + n^k - n^* - p^k + p^*, \quad (3.1)$$

where  $n^k = e^{V^k} u^k$  and  $p^k = e^{-V^k} v^k$ .

REMARK 3.3. To ensure the global convergence of this algorithm one needs to use an appropriate step-size rule, i.e., the last step has to be modified by

$$W^k = W^{k-1} - \tau \left( \frac{1}{\epsilon} \mu_6^k + W^{k-1} \right),$$

where  $\tau > 0$  is a suitable damping parameter. The proof of global convergence follows then exactly the general structure in [7].

#### 4. Numerical results

The performance of the above iterative procedure is tested for various realistic devices. In particular, we consider the standard np-diode, an npn-diode, a unipolar ballistic diode, which can be seen as a simple model for the channel in a MESFET device [22], and finally a realistic setup for a MOSFET — currently the most widely used device type. For all the numerical experiments we use the the forward-bias scaling of the equations (cf. [18]). The dimensionless scaled constants are chosen according to the physical parameters of silicon, which can be found in Table 4.1. In all cases the cost functional is given by (2.10), where  $Q$  is defined by (2.2) with  $Q_1$  and  $Q_2$  as in (2.6) and (2.7), respectively.

The drift-diffusion system and the linear elliptic equations arising during the iterative solution of the optimization problem are discretized via an exponentially fitted scheme of Scharfetter-Gummel type (cf. [5]), which is well-known in semiconductor device simulation. We choose a uniform spatial grid with grid spacing  $h = 1/300$ . All one dimensional examples have been implemented within the software system MATLAB. The Mosfet simulations have been calculated using the finite element software Netgen/NGSolve by Joachim Schöberl.

Parameter	Physical Meaning	Numerical Value
$q$	elementary charge	$1.6 \cdot 10^{-19}$ As
$n_i$	intrinsic density	$10^{10}$ cm <sup>-3</sup>
$\epsilon_S$	permittivity constant	$10^{-12}$ As V <sup>-1</sup> cm <sup>-1</sup>
$\mu_0$	low field mobility	$1.5 \cdot 10^3$ cm <sup>2</sup> V <sup>-1</sup> s <sup>-1</sup>
$U_T$	thermal voltage at $T = 300$ K	0.0259 V

TABLE 4.1. *Physical parameters for silicon.*

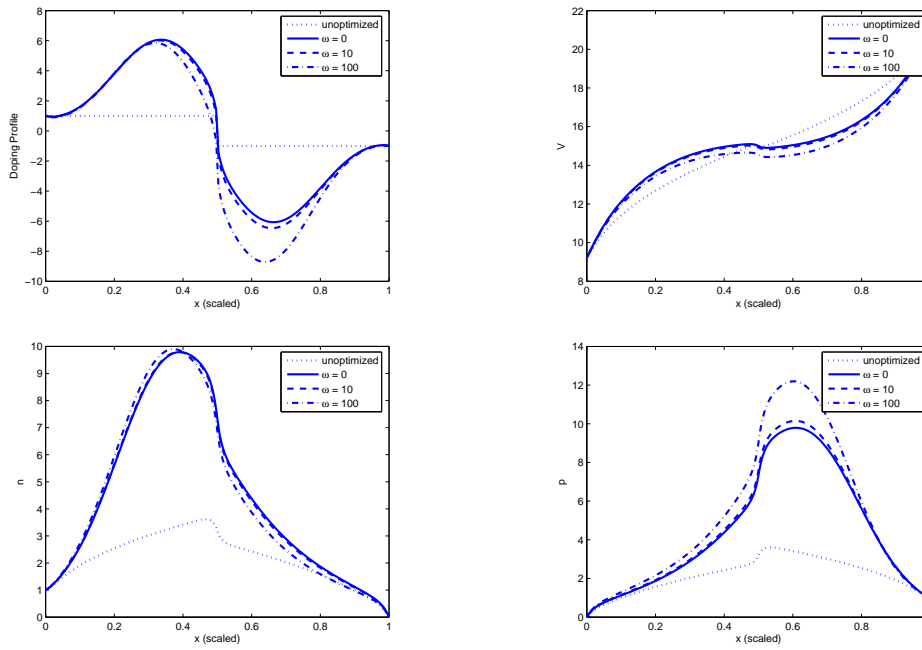


FIG. 4.1. Optimized doping profile (upper left), potential (upper right), electron density (lower left), and hole density (lower right) for the on-/off-state design of a np-diode

**4.1. NP-diode.** Our first example is a standard bipolar np-diode, which is characterized by a doping profile which has exactly one positive and one negative region. The easiest choice incorporating all its characteristics is given by a piecewise constant (scaled) doping profile which jumps abruptly from the value 1 to  $-1$ . This initial profile is shown as the dotted function in figure 4.1. The spatial domain  $\Omega$  is scaled to the unit interval  $(0,1)$ .

The device is further characterized by its nondimensional constants. The Debye length in this experiment is given by  $\lambda^2 = 10^{-3}$  and the scaled intrinsic density is set to  $\delta^2 = 10^{-4}$ . We choose a large applied voltage, i.e.,  $U = 30 \cdot U_T (=0.78V)$ , such that the two design goals are competitive.

The optimization objective is to increase the current flow (i.e., the current flow density, which is constant in the domain since  $J_x = 0$ ) by 50%, while the initial slope of current-voltage characteristics (IVC) is kept small. Consequently, we chose

$$I^* = 1.5 \cdot \int_{\Gamma} J_0 \cdot d\nu, \quad (4.1)$$

where  $\Gamma = \{0\}$  and  $J_0$  is the current flow density obtained with the initial doping.

The regularization is weighted by  $\epsilon = 10^{-1}$  and we compute solutions for different choices of  $\omega = 0, 10, 100$  (used in (2.2)). Furthermore, we choose a relaxation parameter  $\tau = 10^{-1}$ .

The numerical results for these choices of  $\omega$  can be found in figure 4.1 and figure 4.2. In figure 4.1 we compare the resulting doping profiles, the electrostatic potential as well as the electron and hole densities. Also, for reference the respective initially

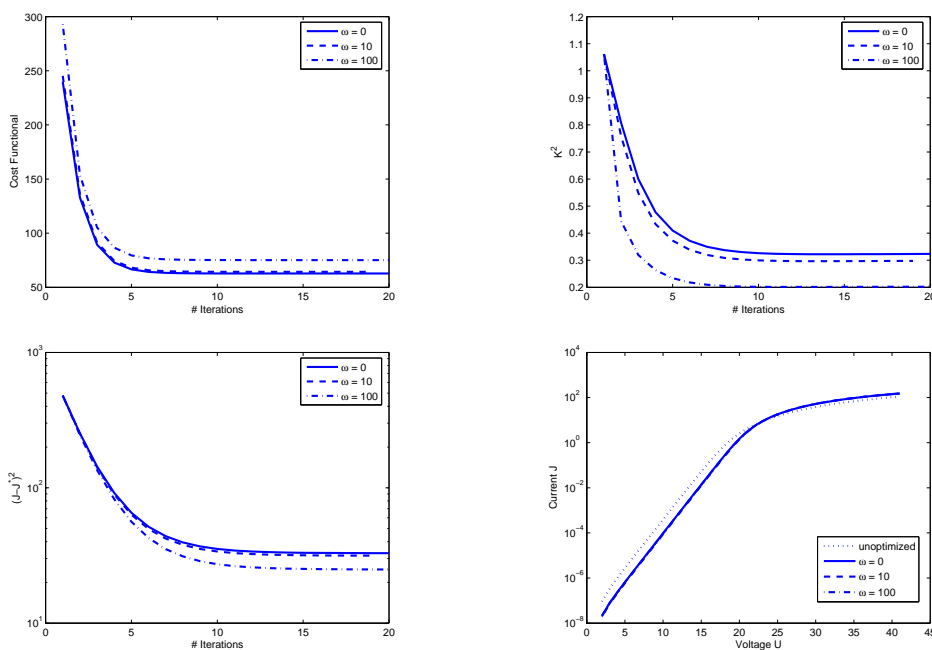


FIG. 4.2. Cost functional (upper left), slope observation (upper right), current observation (lower left), and current-voltage characteristics (lower right) for the on-/off-state design of a np-diode

unoptimized states are presented. The choice  $\omega = 0$  corresponds to the well-known on-state device optimization (cf. [6, 12]) without additional constraint. The effect of the combined on-/off-state optimization is clearly most pronounced for  $\omega = 100$ . Here, the optimized doping profile differs significantly in the p-region where the doping concentration is increased, while the shape in the n-region is almost unchanged in comparison to the on-state optimization. This results in a larger hole density in the p-region.

In all cases we achieve an increase of the on-state current by approximately 30%, as can be seen from figure 4.2. Here, we present the evolution of the cost functional during the iteration, the two observations  $(I - I^*)^2$  and  $K^2$ , respectively, as well as the optimized current-voltage characteristics. While the increase of  $\omega$  has almost no influence on the optimized on-state current, we get the expected decrease of the slope  $K$ . Despite of a decrease by approximately 30% for  $\omega = 100$ , this results in almost no change of the IVC. This can be explained by the fact that the IVC of the np-diode is an exponential function, which immanently has a very small slope in the off-state.

The performance of the generalized Gummel iteration for the multi-objective design problem is comparable to the one for the sole on-state design, which can be seen from the evolution of cost functional in figure 4.2. Note that the algorithm needs approximately 10 iterations to reach the desired minimum.

**4.2. NPN-diode.** The second numerical example is a bipolar npn-diode. Compared to Example 4.1 we use a slightly different parameter set, to get a more pronounced effect of the multi-objective approach. In particular, we choose  $\lambda^2 = 10^{-2}$ ,

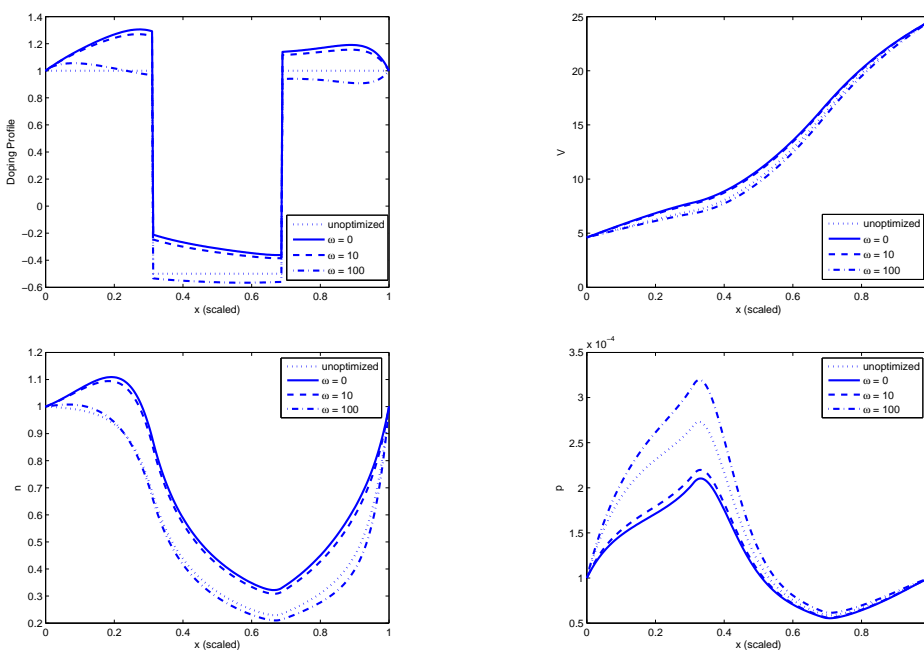


FIG. 4.3. *Optimized Doping Profile (upper left), potential (upper right), electron density (lower left), and hole density (lower right) for the on-/off-state design of a npn-diode*

$\delta^2 = 10^{-2}$  and  $U = 20U_T$ , while  $\epsilon$  and  $\tau$  are unchanged. The parameter range for the objective is the same as above. The initial doping profile is a piecewise constant function taking the values one at the source and drain, and minus one half in the channel; it is shown as the dotted function in figure 4.3.

Again, we present for reference the optimal doping profile for the sole on-state design ( $\omega = 0$ ). Furthermore, the electrostatic potential and the respective electron and hole densities are depicted in figure 4.3. Note that a small weight ( $\omega = 10$ ) has only a negligible influence compared to the on-state design. Here, the increase of the current is achieved by a stronger doping in the n-region. Nevertheless, we get a decrease of the slope  $K$  and still an increase of the on-state current by approximately 30%, as can be seen from figure 4.4.

For a larger, dominant weight ( $\omega = 100$ ) this changes drastically. Now, we see a decrease in the n-regions, while the p-region gets a stronger doping. This results, in fact, in a decrease of the on-state current, while the slope  $K$  is reduced significantly. The corresponding IVCs can be found in figure 4.4. Again, the convergence of the algorithm is very fast, since only 15 iterations are needed to compute the minimizer.

**4.3. Ballistic diode.** The last one dimensional example is an unipolar ballistic diode with a channel doping which is smaller by three orders of magnitude than the source and drain doping; it is depicted as the dotted line in figure 4.5. We use the same cost functional and almost the same parameters as in Example 4.1; only the applied voltage is set to  $U = -20U_T$ .

The computed optimal doping profiles, electrostatic potentials, and electron densities are presented in figure 4.5. As for the on-state design ( $\omega = 0$ ), the increase of

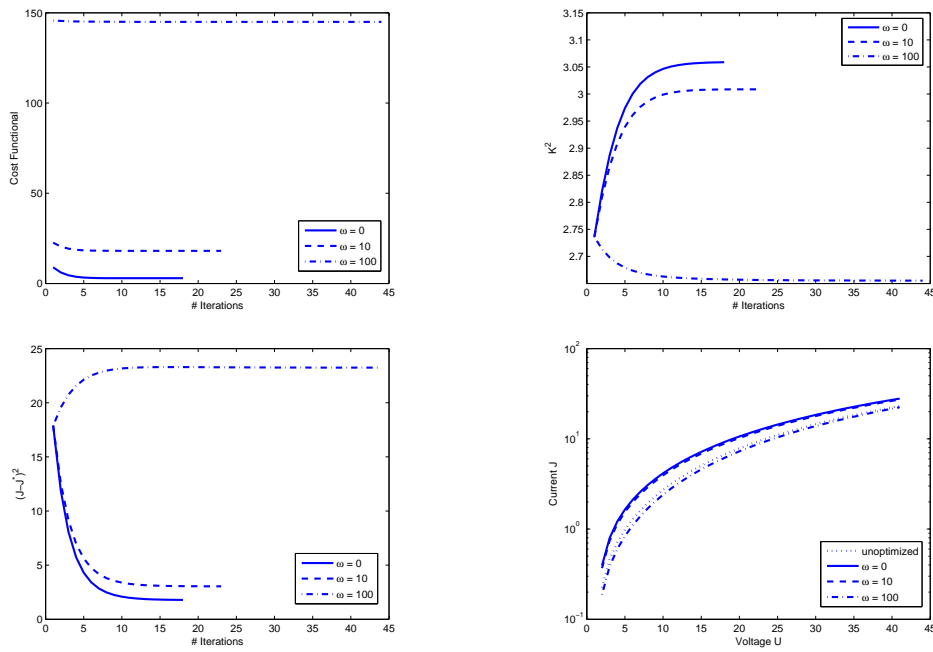


FIG. 4.4. Cost functional (upper left), slope observation (upper right), current observation (lower left), and current-voltage characteristics (lower right) for the on-/off-state design of a npn diode

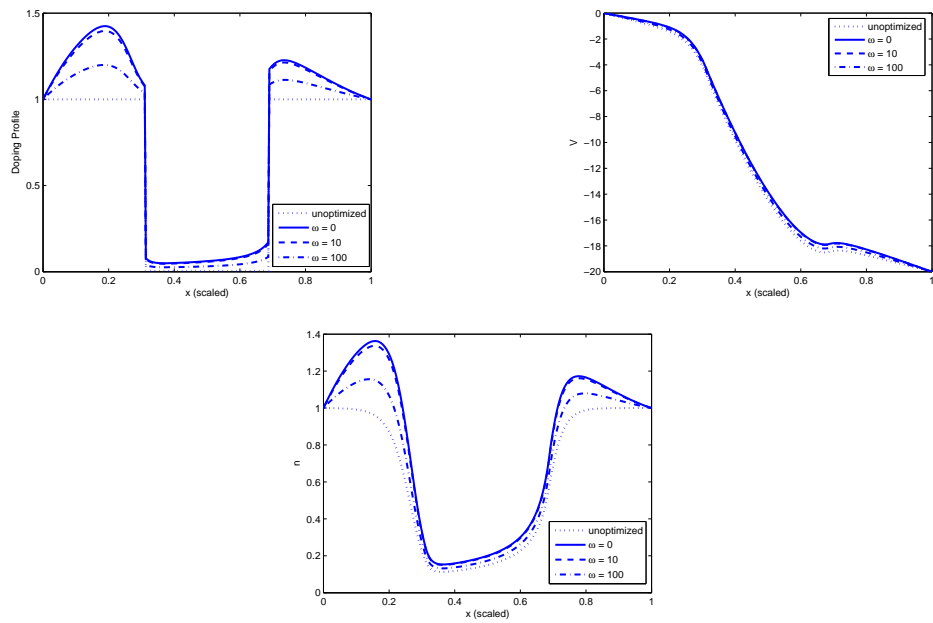


FIG. 4.5. Optimized doping profile (upper left), potential (upper right) and electron density (lower left) for the on-/off-state design of a ballistic diode

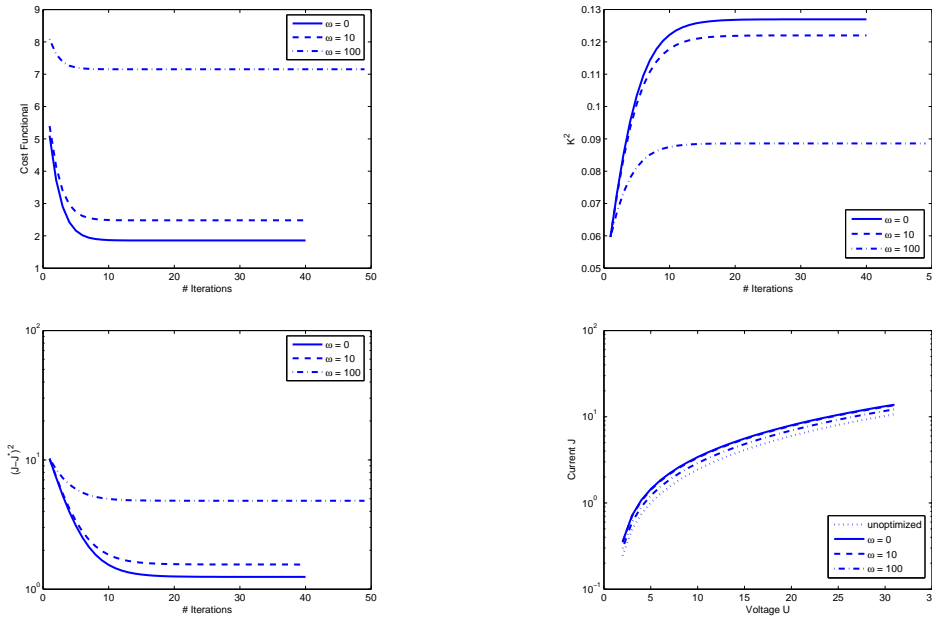


FIG. 4.6. Cost functional (upper left), slope observation (upper right), current observation (lower left) and current-voltage characteristics (lower right) for the on-/off-state design of a ballistic diode

the on-state current is achieved by an increase of the doping density. Increasing the weight  $\omega$  yields a smaller doping in the source and drain regions, such that the current goal is less accurately achieved (see figure 4.6). The effect on the slope is as expected; for  $\omega = 100$  we get a decrease of approximately 30% compared to the on-state design. The price is a reduced on-state current, which is only increased by around 10%. The corresponding IVCs can be found in figure 4.6. As in the other examples we have a fast convergence of the generalized Gummel iteration, such that the minimizer is reached already after approximately 20 iterations.

**4.4. MOSFET.** Finally we present numerical experiments for a MOSFET (metal-oxide semiconductor field-effect transistor) of size  $400 \times 400$  nm (see figure 4.7). The initial doping profile is given by the step function

$$C(x) = \begin{cases} 10^{15} \text{ cm}^{-3} & \text{in } n^+ \text{ region} \\ -10^{13} \text{ cm}^{-3} & \text{in } p \text{ region.} \end{cases}$$

The typical length is set to  $L = 400$  nm, the maximum doping concentration to  $C_{max} = 10^{15}$ . Then the effective parameters are  $\delta^2 = 10^{-5}$  and

$$\lambda^2 = \begin{cases} 0.1 & \text{in silicon} \\ 0.25 & \text{in the oxide layer.} \end{cases}$$

We denote the interface between the silicon and the oxide by  $\Gamma_I$ . The electrons and holes cannot penetrate the oxide layer, therefore they do not need to be computed

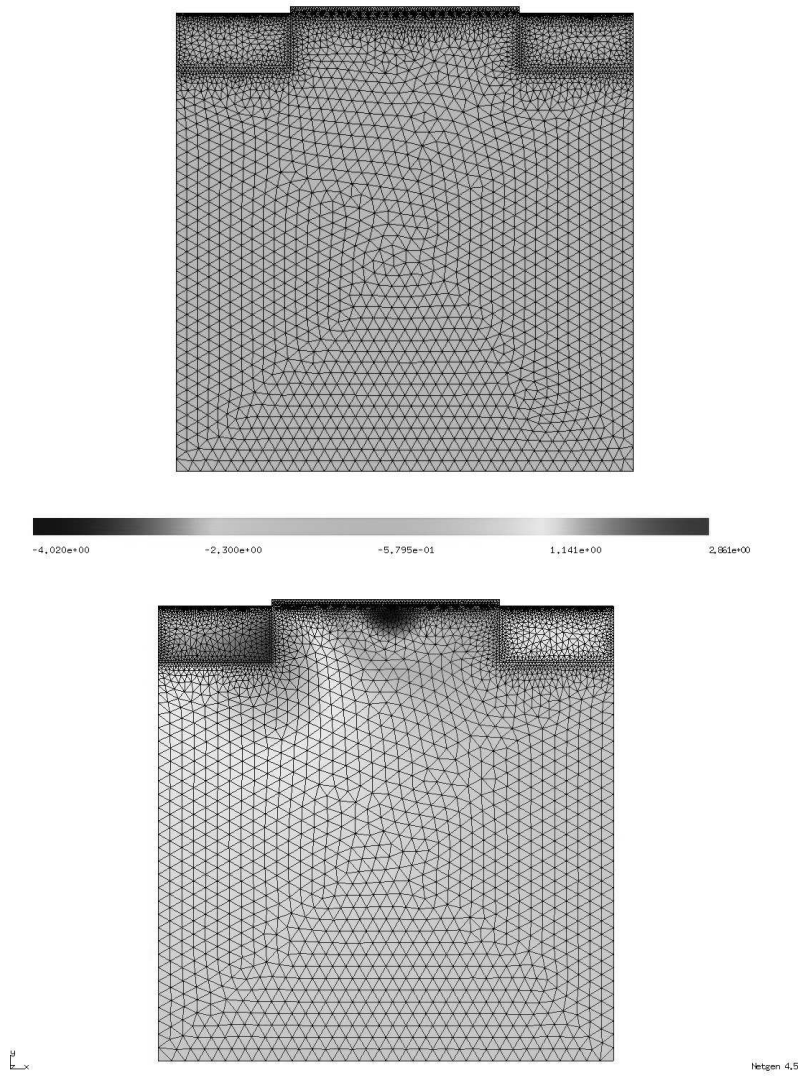


FIG. 4.7. *Mosfet geometry (top) and optimized doping profile (bottom)*

inside the oxide layer. Source, gate and drain correspond to Ohmic contacts, the boundary condition for the potential at the gate contact is given by

$$V_G = -U_F + \phi_G + U_G,$$

where  $\phi_G$  denotes the metal-semiconductor work function difference,  $U_F$  is the flat band voltage, and  $U_G$  is the applied gate potential. We choose the following applied

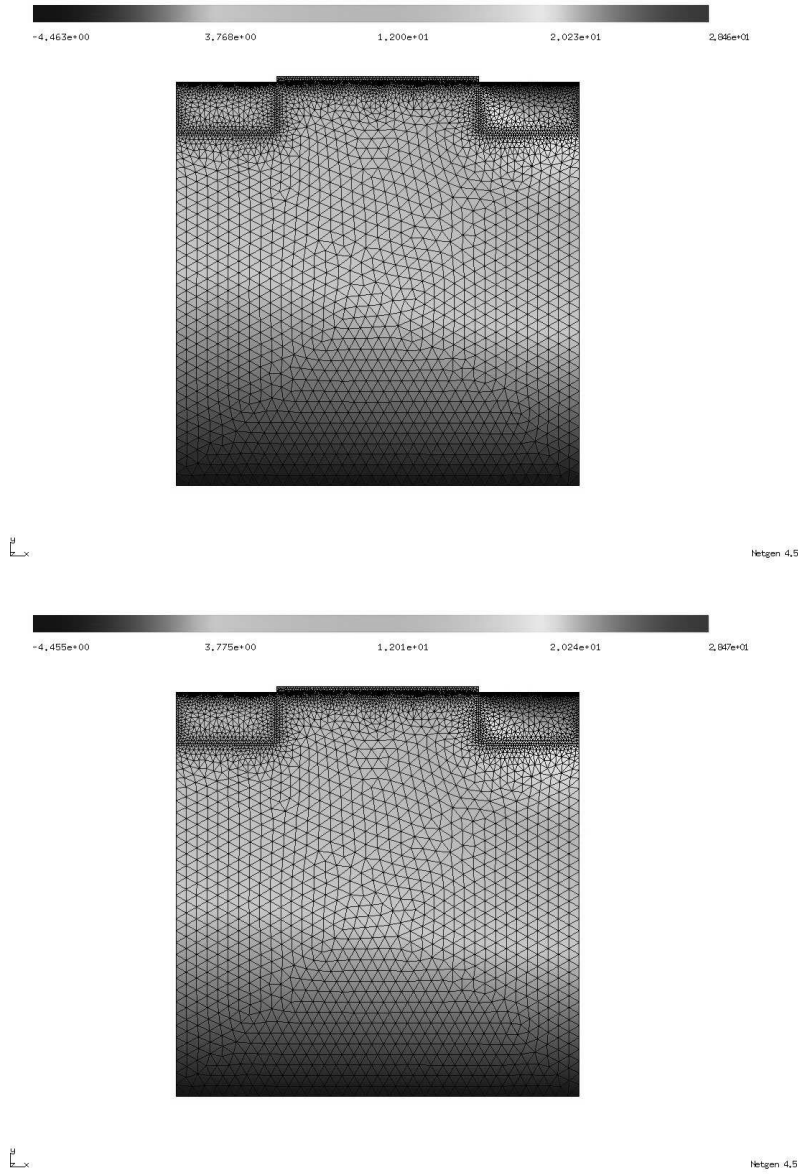


FIG. 4.8. *Potential for initial (top) and optimized doping profile (bottom)*

voltages

$$U = \begin{cases} 0.5 \text{ V} & \text{at the drain,} \\ 0.65 \text{ V} & \text{at the gate,} \\ 0 \text{ V} & \text{at the source.} \end{cases}$$

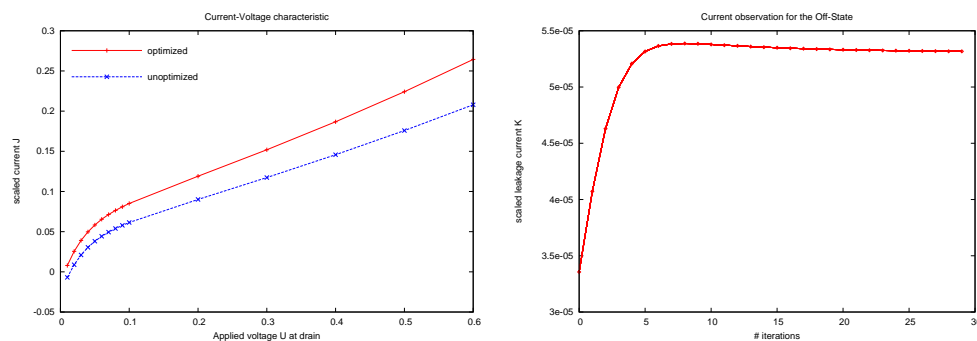


FIG. 4.9. Current voltage curve for optimized and unoptimized doping profile (left) and evolution of the leakage current (right)

We solve the initial system (drift-diffusion equations with profile  $C^*$  in order to obtain  $V^*$ ) using a stabilized mixed finite element discretization [5]. The optimality system is discretized using piecewise linear basis functions. The domain is discretized into 8570 triangles (see figure 4.7).

Here we present results for the parameters  $\epsilon = 10^{-4}$  and  $\omega = 10^3$ , and the damping parameter  $\tau = 10^{-1}$ . The competition of the two design goals in the MOSFET case is more pronounced, since the initial slope of the IVC is steeper. In this case the slope  $K$  in the off-state increases by almost 50%, while the on-state current can only be increased by about 20%. The potential of the initial and optimized doping profile can be seen in figure 4.8, the optimal doping profile in figure 4.7. The increase of the on-state current by 20 % and the evolution of the leakage current  $K$  during the optimization procedure can be seen in figure 4.9.

**Acknowledgments.** Financial support is acknowledged by the DFG via SPP 1253, the DAAD/Vigoni programme, and the Austrian Science Foundation FWF via SFB F 013/08.

#### REFERENCES

- [1] F. Brezzi, L.D. Marini and P. Pietra *Two-dimensional exponential fitting and applications in drift-diffusion models*, SIAM J. Numer. Anal., 26, 1342–1355, 1989.
- [2] M. Burger, H.W. Engl, P. Markowich and P. Pietra, *Identification of doping profiles in semiconductor devices*, Inverse Problems, 17, 1765–1795, 2001.
- [3] M. Burger, H.W. Engl and P. Markowich, *Inverse doping problems for semiconductor devices*, T.F. Chan, Y. Huang, T.Tang, J.A. Xu and L.A. Ying, eds., *Recent Progress in Computational and Applied PDEs*, Kluwer, Boston, Dordrecht, London, 39–54, 2002.
- [4] M. Burger, M. Hinze and R. Pinnau, *Optimization models for semiconductor dopant profiling*, C. Cercignani and E. Gabetta eds., *Transport Phenomena and Kinetic Theory: Applications to Gases, Semiconductors, Photons, and Biological Systems*, Birkhäuser, Boston, 2006.
- [5] M. Burger and R. Pinnau, *Exponential fitting for adjoint equations in semiconductor design*, in preparation.
- [6] M. Burger and R. Pinnau, *Fast optimal design of semiconductor devices*, SIAM J. Appl. Math., 64, 108–126, 2003.
- [7] M. Burger and R. Pinnau, *A globally convergent Gummel map for optimal dopant profiling*, M3AS, to appear, 2008.
- [8] C.R. Drago, *On fast optimal control for energy-transport-based semiconductor design*, Mathematics in Industry 11, Springer, Berlin, 347–355, 2007.

- [9] C.R. Drago and A.M. Anile, *An optimal control approach for an energy transport model in semiconductor design*, Proceedings SCEE 2004, Mathematics in Industry, Springer Verlag, 2004.
- [10] C. Drago, R. Pinnau, *Optimal dopant profiling based on energy-transport semiconductor models*, M3AS, 18(2), 195–214, 2008.
- [11] H.K. Gummel, *A self-consistent iterative scheme for one-dimensional steady state transistor calculations*, IEEE Trans. Elec. Dev., ED-11, 455–465, 1964.
- [12] M. Hinze and R. Pinnau, *Optimal control of the drift-diffusion model for semiconductor devices*, K.H. Hoffmann, I. Lasiecka, G. Leugering and J.Sprekels, eds., Optimal control of complex structures, ISNM, Birkhäuser, 139, 95–106, 2001.
- [13] M. Hinze and R. Pinnau, *An optimal control approach to semiconductor design*, Math. Mod. Meth. Appl. Sci., 12, 89–107, 2002.
- [14] M. Hinze and R. Pinnau, *A second order approach to optimal semiconductor design*, JOTA, 133(2), 179–199, 2007.
- [15] M. Hinze and R. Pinnau, *Mathematical tools in optimal semiconductor design*, Bulletin of the Institute of Mathematics, Academia Sinica (New Series), 4(2), 569–586, 2007.
- [16] S. Holst, A. Jüngel and P. Pietra, *A mixed finite-element discretization of the energy-transport model for semiconductors*, SIAM J. Sci. Comput., 24, 2058–2075, 2003.
- [17] P.A. Markowich, *The Stationary Semiconductor Device Equations*, Springer, Wien, New York, 1986.
- [18] P.A. Markowich, C.A. Ringhofer and C. Schmeiser, *Semiconductor Equations*, Springer, Wien, New York, 1990.
- [19] M.S. Mock, *Analysis of Mathematical Models of Semiconductor Devices*, Boole Press, Dublin, first edition, 1983.
- [20] R. Plasun, M. Stockinger, R. Strasser and S. Selberherr, *Simulation based optimization environment and its application to semiconductor devices*, Proceedings IASTED Intl. Conf. on Applied Modelling and Simulation, 313–316, 1998.
- [21] Y. Sawaragi, H. Nakayama and T. Tetsuzo, *Theory of Multiobjective Optimization*, Academic Press, Orlando, 1985.
- [22] S. Selberherr, *Analysis and Simulation of Semiconductor Devices*, Springer, Wien, New York, 1984.
- [23] M. Stockinger, *Optimization of ultra-low-power CMOS transistors*, PhD Thesis, Technical University Vienna, 2000.
- [24] M. Stockinger, R. Strasser, R. Plasun, A. Wild and S. Selberherr, *A qualitative study on optimized MOSFET doping profiles*, Proceedings SISPAD 98 Conf., Leuven, 77–80, 1998.
- [25] M. Stockinger, R. Strasser, R. Plasun, A. Wild and S. Selberherr, *Closed-loop MOSFET doping profile optimization for portable systems*, Proceedings Intl. Conf. on Modeling and Simulation of Microsystems, Semiconductors, Sensors, and Actuators, San Juan, 411–414, 1999.
- [26] G.M. Troianello, *Elliptic Differential Equations and Obstacle Problems*, Plenum Press, New York, first edition, 1987.
- [27] W.R. Van Roosbroeck, *Theory of flow of electrons and holes in germanium and other semiconductors*, Bell Syst. Tech. J., 29, 560–607, 1950.
- [28] M.T. Wolfram, *Inverse dopant profiling from transient measurements*, J. Comput. Electronics, 4, 409–420, 2007.